

Linear Motor for Multi-Car Elevators: Design and Position Measurement

Cagri Gurbuz, Ender Kazan, Ahmet Onat and Sandor Markon

Abstract—Multi-car elevator is an emerging technology consisting of two or more elevator cars moving independently in an elevator hoistway, which has become more appealing as building heights increase. In this paper, the design and drive methodologies for a linear motor driven multi-car elevator system with independently moving cars is introduced together with experimental results. Additionally, a safety method developed for the linear motor elevator and the conditions necessary for its proper operation are discussed. The new results introduced in this paper are in the areas of the design method of the linear motor for multi-car elevator system, and the preliminary results for the position measurement system.

Keywords: Linear motors, elevators, safety methods, design optimization, position measurement

I. INTRODUCTION

Recent improvements in building technology has made it possible to increase heights considerably, with the current highest building in the world being higher than 800m. Although structural requirements are great in erecting such buildings, another very important aspect is one of logistics; i.e., how to allow for transport of goods and waste, of supplies such as energy and water and also of people into and out of the building, since the ratio of building volume to the area of transport passages diminishes. The transport passages mainly consist of elevator hoistways, and there can be a large number of dedicated hoistways in tall buildings, 50 being not uncommon.

One of the main criteria for elevator performance is passenger hall-waiting time. To improve this performance several techniques such as express elevators which only serve specific floors or building sections are employed. However, as long as one elevator car is installed in a hoistway, these solutions give limited performance. One of the promising solutions is to install a large number of elevator cars in every hoistway (which may not overtake cars in front of themselves), and control them using a sophisticated group control algorithm [1]–[4]. The conventional elevator mechanisms relying on ropes, pulleys and counterweights have limitations on the number of cars that can be placed in the same hoistway. Therefore a new method, such as linear motor driven elevator cars is needed [5].

The research on linear motors is new compared to rotational machines [6], and generally is handled in contexts where weight of the mover is not critical to performance which simplifies the design requirements and analysis. Recently however,

linear motors for drive of vertical loads in transportation have been also studied [7]–[10] where high thrust to weight ratio is required. A strong candidate is permanent magnet linear synchronous motors (PMLSM), which has become feasible in the recent years with the advances in permanent magnet technology where high coercivity permanent magnet material with low cost has become available [8], [9], [11]–[13].

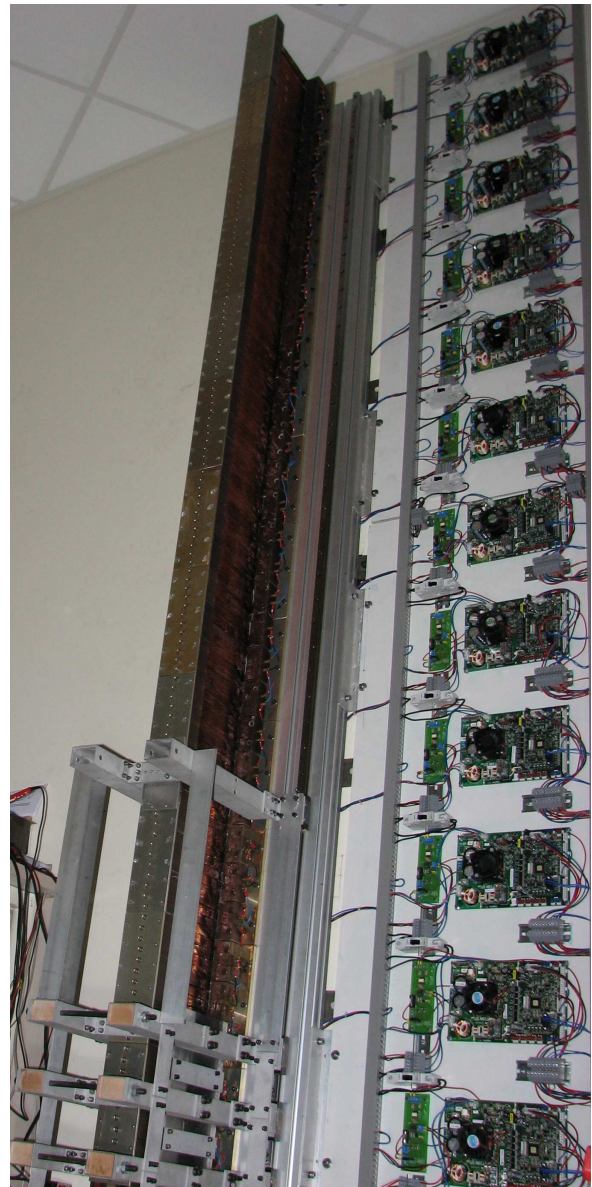


Figure 1. The linear motor designed for multi-car elevator applications.

In multi-car elevator applications the elevator car must be free of any connections, mechanical or electrical, to facilitate freedom in motion. This brings some interesting design requirements where safety devices, position encoding, supplying power to car interior, communication of call buttons etc. must all be implemented externally, from the stator side. All of these must be solved satisfactorily before successful designs can be produced. This constraint also mandates that the design must be a long armature type where the stator contains the coils and the mover contains permanent magnets.

In this paper, we describe the main features of a linear motor designed for vertical transportation applications, including safety [14], [15]. Then the optimization method used to design the new generation mover is introduced. Next we introduce a novel active position measurement method, where the stator itself is used to determine the position of the mover which will be used for controlling at low speeds. Finally results of tests performed on the actual full scale motor are given.

II. SAFETY SYSTEM FOR LINEAR MOTOR ELEVATORS

Although the mover can be held stationary using electromagnetic force, an electromechanical brake for arresting the mover while the elevator is stopped at a floor is also necessary. However, because of the design requirement that no electrical connections must be made to the elevator car, such a device cannot be installed on the mover itself, but must be on the stator side. A simple but expensive implementation is to build a solenoid operated brake with a length equal to the length of the stator.

Another solution is to re-design the stator and motor drive method such that its functionality is extended beyond only thrust generation, to also generate a virtual current vector along the top edge of the stator. This can then be exploited on the mover by a suitable magnetic device to generate a sideways force and drive a brake mechanism.

Special DC bias currents superposed on the drive currents can be used to generate a virtual brake current along the top edge of the stator which cause a force on a permanent magnet in its vicinity (Fig. 2). The permanent magnet is in turn connected to a brake mechanism. The electromechanical structure of the brake is such that in the absence of the DC bias currents, the brake is engaged and in their presence the brake is released. Using this method it becomes possible to generate thrust and operate the brake mechanism on the same part of the motor section [15]. Such a brake mechanism can also be used to create safety zones on the elevator system, in which brakes will be applied to an elevator car and stopped unless the car has permission to transit a given section of the stator.

The stator winding pattern required to generate the virtual current vector at the top edge of the stator will be explained next. The relationship of this current to the DC bias currents depends on the winding pattern of the motor. We employ a winding pattern which we will call here “balanced winding”, consisting of coils where each phase is arranged at 120° electrical degrees as shown in Fig. 3. For the balanced winding and the conventionally defined motor phase currents i_a , i_b , i_c ,

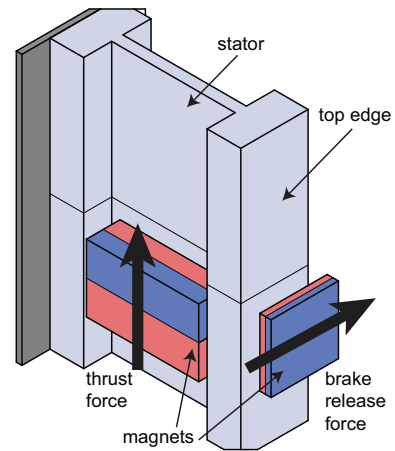


Figure 2. Generation of thrust and brake force on the same section of the stator.

where $i_a(t) + i_b(t) + i_c(t) = 0$ under normal drive conditions, the virtual current vector at the top edge of the stator becomes zero over a distance of one phase length. However, if the neutral point of the motor is tapped to sink a DC current component through all phase coils which we call the brake current I_{brake} , then the virtual current becomes non-zero for any value of I_{brake} .

$$I_{brake} = i_a(t) + I_{DC} + i_b(t) + I_{DC} + i_c(t) + I_{DC} \quad (1)$$

where I_{DC} is the bias current injected through each phase of the motor, and $I_{brake} = 3I_{DC}$. It becomes possible, therefore, to implement a motor where the brake current can be applied independently of the drive currents.

In the industry, the preferred winding pattern is what we call “segmented winding” where two phases are arranged with 120° electrical degrees, but the third phase with 60° , and fed a reversed current, Fig. 3. This pattern is advantageous because the motor can be divided into segments, thus it is simpler to manufacture. However, when driven by balanced currents, the stator top edge current for the segmented winding is non-zero. If the motor neutral point is tapped, it can be driven to zero only for some special case bias currents.

The balanced winding is better suited for a safety brake operation on linear motor elevators since generating a stator top field requires a special current pattern. The segmented winding on the other hand, will generate a zero stator top field in one special case current. In case of emergency where the motor or the motor driver is damaged or power is lost, there is a larger set of possible failure modes in which the balanced winding will not be able to provide the special current pattern and thus the brake will engage to arrest the fall of the elevator car. Another advantage of balanced winding is that since the system is set up in such a way that brake is engaged for zero brake current and disengaged when brake current exceeds a certain value, there is no need to supply brake current when the elevator car must be stopped [15].

III. OPTIMIZATION METHOD USED TO DESIGN THE MOVER

For the air-core linear PM synchronous motor, a mover with iron yoke and permanent magnets is investigated as shown in

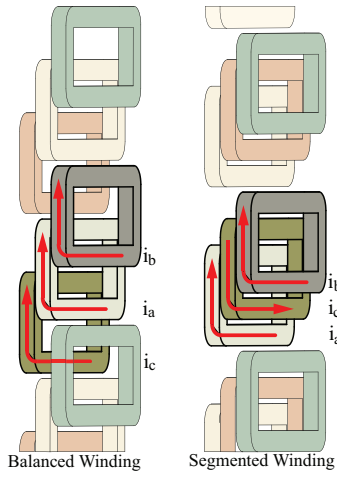


Figure 3. Winding patterns of linear motor stators.

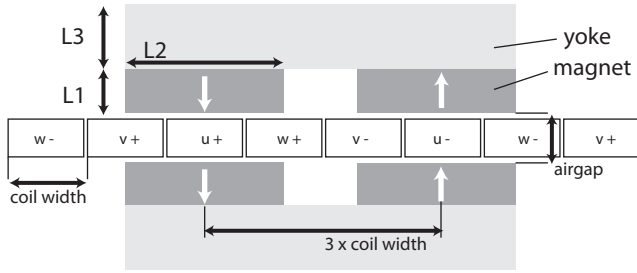


Figure 4. Cross section of examined yoke-type mover.

Figure 4. All of the dimensions which are the thickness of the magnet L_1 , the width of the magnet L_2 , and the thickness of the yoke L_3 are treated as design variables. In general, thrust force is chosen as one of the optimization objectives for linear motors, however we choose payload instead of thrust force as objective since the motor is designed for vertical transportation where how much load can be lifted is more important than how much force can be obtained. Consequently, the objectives of this optimization are chosen as high payload P , low force ripple r_d , low magnet weight Q and low brake effect e_b described in Equations 2, 3, 4, 5.

$$P = F - Q \quad (2)$$

$$r_d = r_d = (F_{x_{max}} - F_{x_{min}}) / F_{x_{ave}} \times 100 \quad (3)$$

$$e_b = (F - F_b) / F \times 100 \quad (4)$$

$$Q = d_m \times V_m \quad (5)$$

where F is the thrust force, Q is the total weight of one mover, $F_{x_{max}}$, $F_{x_{min}}$ and $F_{x_{ave}}$ are the maximum, the minimum and the average forces within the movement of one phase distance respectively. F_b is the thrust force at the instant when the DC brake currents together with the AC drive currents are applied as described in Section II. Density and volume of the magnets are shown as d_m and V_m respectively.

For the optimization, the variables are bounded as $10 \leq L_1 \leq 40$, $20 \leq L_2 \leq 60$ and $10 \leq L_3 \leq 40$ in mm. Instead of defining a continuous problem space including all

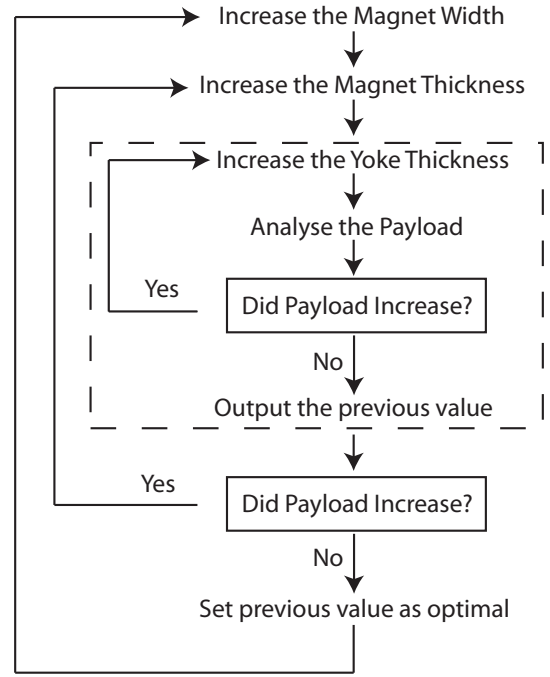


Figure 5. Finding optimal magnet and yoke thicknesses regarding to payload.

of the three variables, an alternative procedure is followed where first L_1 and L_3 are optimized while holding L_2 fixed at different values. Namely, for each L_2 value, the values for L_1 and L_3 that give the highest payload are found. Then, by comparing the performance on all the objectives at different values, the optimum value for L_2 is found. The main advantage of this procedure is reduced search space and prioritizing high payload over other objectives. The reason for optimizing L_2 variable after L_1 and L_3 is its higher effect on all of the objectives. The search algorithm to determine the thickness of magnet, L_1 , and yoke, L_3 , is given in Figure 5. For a given L_1 and L_2 , the thickness of the yoke (i.e. L_3) can be increased as long as there is still increase in payload. Although larger yoke thicknesses after this point give higher thrust forces, we define this point as the optimal value since the increase in weight of the mover is larger than the increase in thrust force which is not desirable for higher payload objective. Similarly, the same algorithm can be applied for determining the optimal value of magnet thickness L_1 . However, there is still need to determine optimal L_3 again for each L_1 to be compared. The optimal L_1 and L_3 values calculated for each L_2 are given in Table I.

Table I
OPTIMAL VALUES OF L_1 AND L_3 WITH RESPECT TO L_2

L_2 (mm)	20	24	28	32	36	40	44	48	52	56	60
L_1 (mm)	34	30	30	30	28	28	28	28	28	30	28
L_3 (mm)	12	14	16	18	20	22	24	24	24	24	22

Once the optimal values of magnet and yoke thicknesses (L_1 and L_3) are determined, the objectives can be analyzed for comparison of magnet width L_2 to find the final optimal solution. The results of objectives with respect to L_2 variable are found by a 2D FEM software [16] shown in Figure 6. It

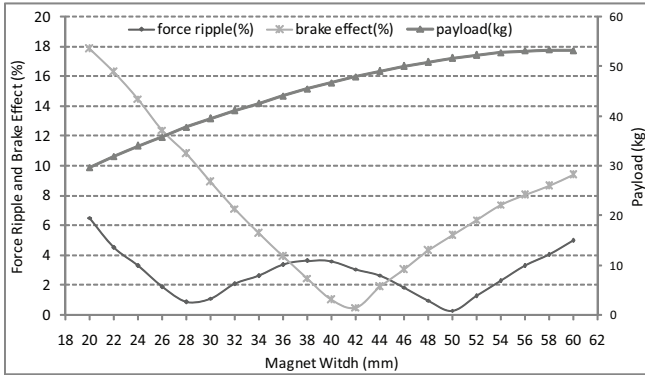


Figure 6. Change of objectives vs magnet width.



Figure 7. Final coil shape used for the stator.

can be seen that all of the objective functions have different trends over L_2 . Therefore, there is need for a multi-objective optimization with a cost function which can be defined as,

$$W_{mw} = k_1 W_1 + k_2 W_2 + k_3 W_3 + k_4 W_4 \quad (6)$$

where,

$$W_1 = e_b \quad (7)$$

$$W_2 = r_d \quad (8)$$

$$W_3 = 1/P \quad (9)$$

$$W_4 = Q \quad (10)$$

In the cost function, it is important to reduce W_3 and W_4 in order to reduce the running costs and initial costs respectively. On the other hand, it is also important to reduce W_1 and W_2 for the sake of controllability. Therefore, $k_1 \dots k_4$ can be chosen with respect to the desired weights of costs and controllability of the motor [17].

IV. IMPLEMENTATION OF THE LINEAR MOTOR

The stator coil shape is important in the implementation of the linear motor. It defines the performance of the motor including the brake and thrust forces, and also the cost of the completed unit based on its complexity. Here the design for the full scale experimental test motor and its special driver topology will be explained.

Several coil shapes were considered for the stator. Although initial designs consisted of complex shaped coils with different shapes for each phase, final design shown in Fig. 7 was eventually reached. It consists of a simple, single coil shape repeated to construct a balanced winding stator.

As discussed in Section II, brake currents must flow into the neutral point of the motor, superposed on the usual balanced

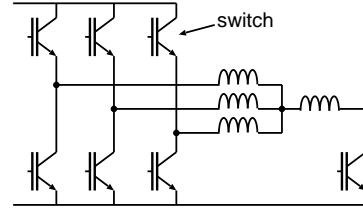


Figure 8. Motor driver, for the brake operation discussed.

drive currents. To make this possible, the neutral point of the motor was connected to ground or DC link, over an extra switch on the motor that we call the “seventh switch” and a ballast inductor, as shown in Fig. 8. To produce brake currents, the mid part of the center aligned PWM cycle when all motor coils are connected to DC link is used. During this time period, the seventh switch is closed for a suitable duration. As another strategy, it is also possible to generate thrust and brake forces using a different part of the stator than that used for thrust generation.

V. POSITION SENSING

It is desirable to drive linear motors with no electrical connections between the mover and stator. However, most position sensing methods available [18] rely on a stationary passive position reference such as the grated strip of an incremental encoder and an active part attached to the mover, where a flexible cable must be connected to the mover of the motor.

In this section, the principle of operation and the methodology of the development and testing of a passive position sensor system that uses one non-active linear motor stator segment in front of or behind the mover will be given. The sensing operates on the principle of measuring the variation of the mutual inductance between different coils of the stator, when a magnetic shunt in the form of ferromagnetic material fixed at a predetermined distance ahead of the mover moves along them. The measurement is sufficiently accurate and reliable to supplement a sensorless position control scheme, as a backup scheme. By combining two completely different position sensing methods, the total system is judged to be safe to be used in a passenger elevator.

When we deliberately introduce physical asymmetry into the system of magnetic circuit of the stator coils, it causes the terminal parameters also to show asymmetrical behavior. We can infer information about the conditions causing the asymmetry, by measuring the terminal parameter values. Let us consider the case of placing a block of soft magnetic material in the vicinity of the linear motor armature winding (Fig. 9). When we apply a sinusoidal current into one phase coil and analyze the field distribution, an asymmetric variation depending on the position of the ferromagnetic block can be clearly seen. The finite element magnetic analysis software “FEMM” [16] was used to analyze the field distribution in a 2-dimensional approximation, the cross section of the stator, to generate Fig. 9, with the ferromagnetic block placed in an asymmetric position. In the following, we call that block a “magnetic shunt”. Since the mover is fixed at a known distance

away from the magnetic shunt, by measuring the position of the shunt, the position of the mover can easily be calculated.

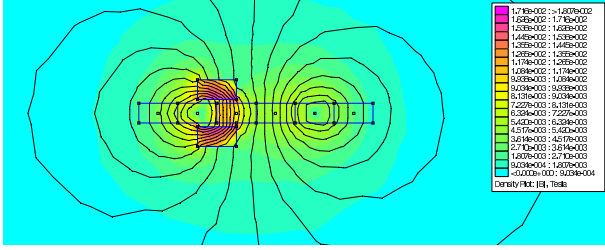


Figure 9. Model of linear motor armature with magnetic shunt, showing cross section through motor coils and shunt.

The method can be analyzed similar to the measurement of mutual inductance between two coils as shown in Fig. 10. When a sinusoidal voltage is applied to one of the coils, the induced voltage at the other side depends on the mutual inductance. The mutual inductance in this case depends, in turn, on the position of the magnetic shunt.

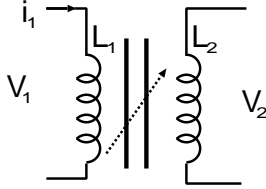


Figure 10. Setup for measuring mutual inductance.

The equations of the circuit are given in Eqs. 11 and 12:

$$V_1 = R_1 i_1 + L_1 \frac{di_1}{dt} + M \frac{di_2}{dt} \quad (11)$$

$$V_2 = R_2 i_2 + L_2 \frac{di_2}{dt} + M \frac{di_1}{dt} \quad (12)$$

From the analysis mentioned above, we can calculate the induced voltages across the two other motor phases for each magnetic shunt position. When we move the magnetic shunt across the length of the armature, these voltages will change accordingly. The expected values of induced voltages can be calculated or measured beforehand, and placed in a look-up table. During the operation, the measured induced voltages can be compared to those in the table, and the position of the magnetic shunt can be found by a search algorithm. Instead of using a ferromagnetic shunt, a diamagnetic shunt can also be used, which would have the reverse effect on breaking the symmetry of the magnetic field.

VI. RESULTS

In this section we present results about the generated brake force, a comparison of the generated thrust force with respect to the simulation results, and the results of the active position sensing method discussed in Section V. The simulated and experimental results are based on the full scale motor designed using the method as described in this paper, except the brake force data, which was generated using an earlier motor, also designed and implemented by the authors.

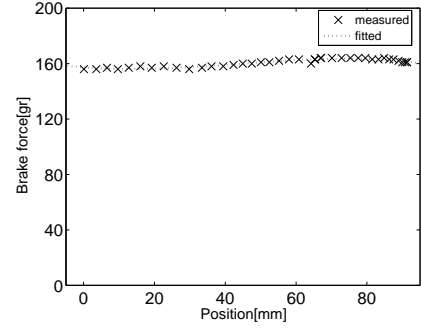


Figure 11. Distribution of brake force.

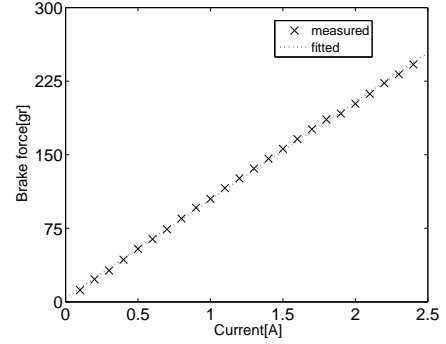


Figure 12. Brake force with respect to brake current.

The brake force should ideally remain constant with respect to mover position, and change linearly with respect to brake current. To measure these performance values, a magnet plate with N38 type magnets was built and mounted on the mover using a linear bearing movable perpendicular to the direction of motion. The sideways force was measured using a strain gage. The position along the stator was measured using a linear position encoder. Brake forces were applied to each coil separately using voltage supplies. The brake force with respect to brake plate position on the stator can be seen in Fig. 11. The brake force does not vary much when the mover advances on the stator. However, the brake force is not large. Therefore a brake system with a carefully designed mechanical advantage is necessary. Also the brake plate magnetic design can be improved to increase the brake force.

In Fig. 12, the change in brake force with respect to brake current while the mover is in a fixed position can be seen. The change in brake force with respect to brake current is linear.

The payload performance of a linear motor for vertical applications is important. A mover was designed according to the method summarized in Section III. The thrust force was measured by applying a current of 3A to the stator and increasing the downward force on the mover while observing the vertical displacement. The mover shifted to a lower position as force is increased, and just after the maximum thrust force, it slips. This test was repeated for two air gap values, 19mm and 14mm. Smaller air gaps are advantageous but may be difficult to obtain due to manufacturing tolerances. The design gap for this motor was 14mm, which includes the thickness of the stator.

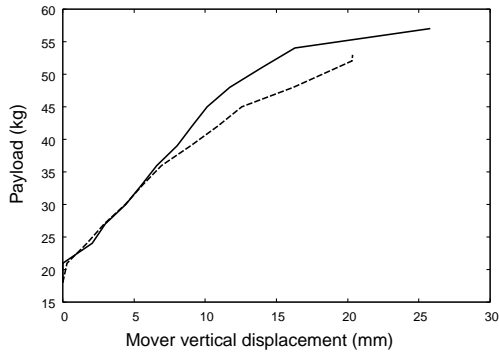


Figure 13. Motor payload for different air gap values for 3A current.

Table II
DIMENSIONS OF THE TESTED MOTOR

Phases	3	
Stator width	200	mm
Stator thickness	10	mm
Pole pitch	60	mm
Width of magnetic shunt	20	mm
Length of magnetic shunt	190	mm
Thickness of magnetic shunt	40	mm

Results of this test can be seen in Fig. 13. The total capability of 19mm mover is 53kg, while for 14mm, it is possible to carry 59kg of weight (since the optimization did not include the dead weight of the mover support structure, it is added to the thrust force). The simulation results show that the same mover should be capable of lifting 54kg for 19mm, and 58kg for 14mm air gaps. These results suggest that this slotless motor design is well suited to 2D FEM analysis. Although the payload capacity of the designed movers is high, the payload can be linearly and inexpensively increased by mechanically connecting several movers together, with one phase length separation [15]. Using such an arrangement, the weight of one person can easily be lifted using three movers.

For position sensing we have tested the method that we described in previous section on a linear motor with dimensions shown in Table II.

One coil of Phase B was fed with $1kHz$ sinusoidal current, and the induced voltages in one coil each of Phase A and Phase C were measured. Since the excitation would cause eddy currents in a solid iron core, a laminated magnetic shunt was used to reduce their effect.

The result shown in Fig. 14 is obtained with a laminated magnetic shunt of iron. For this iron lamination fill factor is 0.9 and the lamination thickness is 1 mm. We have found that the position sensing is feasible.

The locus of the two voltages is shown in Fig. 15. In principle, by measuring the voltages, we can read out the position if this curve is labeled with measured shunt positions.

VII. CONCLUSIONS

In this paper, we describe the main features of a linear motor designed for vertical transportation applications, including safety. Also a mover optimization method for designing the mover is introduced. Depending on the cost function, how

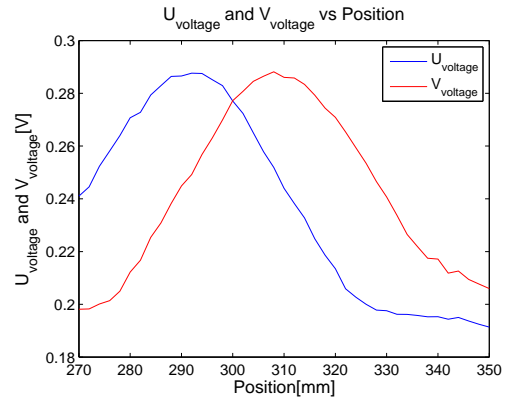


Figure 14. Induced terminal voltages of coil A and C with respect to shunt position.

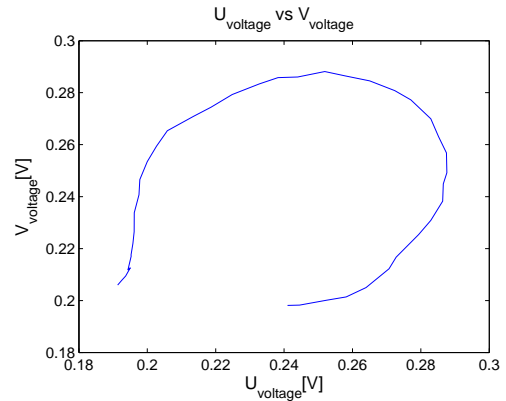


Figure 15. Parametric representation of the data in Fig. 14, showing voltages of coils A and C with respect to each other as shunt is moved.

we can find optimal mover structure for different features (e.g force ripple, payload, thrust force etc.) is explained. Once the optimal parameters of the mover are determined, the importance of the coil shapes for implementation of the linear motor is explained. Also the effect of the coil shape on the brake mechanism is represented. The idea was supported by methodology of new position sensing method followed by simulations and experimental results.

It has been inferred that the linear motor system can operate both propulsion and safety system with different optimization of mover. Further research will be done to operate this system according to the new position sensing method, and thus to satisfy the idea of ropeless linear motor. Furthermore, we are still working on the optimization of mover, position sensing method and safety system.

It has been observed that the proposed system can successfully operate as a combined propulsion and safety system. Further research will be done to validate the operation of the safety system for all failure modes, and thus to satisfy the requirements for certification. Furthermore, we are working on the modification of the optimization procedure to include directly the cost of the stator, which will become an important factor when applying the results of this research to elevators of extreme high-rise buildings.

ACKNOWLEDGMENTS

This research was supported in part by Fujitec Co., Ltd. of Japan.

REFERENCES

- [1] T. Ishii, "Elevators for skyscrapers," *Spectrum, IEEE*, vol. 31, no. 9, pp. 42–46, 1994.
- [2] W. Jones, "How to build a mile-high skyscraper," *Spectrum, IEEE*, vol. 44, no. 6, pp. 52–53, 2007.
- [3] S. Markon, H. Kita, and H. Kise, *Control of Traffic Systems in Buildings: Applications of Modern Supervisory and Optimal Control (Advances in Industrial Control)*. NJ, USA: Springer-Verlag New York, Inc., 2006.
- [4] S. Takahashi, H. Kita, H. Suzuki, T. Sudo, and S. Markon, "Simulation-based optimization of a controller for multi-car elevators using a genetic algorithm for noisy fitness function," in *The 2003 Congress on Evolutionary Computation, CEC '03*, vol. 3, 2003, pp. 1582–1587.
- [5] M. Miyatake, T. Koseki, and S. Sone, "Design and traffic control of multiple cars for an elevator system driven by linear synchronous motors," in *Proc. Symposium on Linear Drives for Industry Applications*, no. AP-22, 1998, pp. 94–97.
- [6] I. Boldea and S. Nasar, *Linear motion electromagnetic devices*. Taylor & Francis, 2001.
- [7] J. F. Gieras and Z. J. Piech, *Linear synchronous motors: transportation and automation systems*. CRC Press, 2000.
- [8] H. Yamaguchi, H. Osawa, T. Watanabe, and H. Yamada, "Power supply of long stator linear motors application to multi mobile system," in *Proc. AMC96*, 1996, pp. 441–446.
- [9] S. Chevallier, M. Jufer, and Y. Perriard, "Linear motors for multi mobile systems," in *IAS2005*, 2005, pp. 2099–2106.
- [10] A. Cassat, B. Kawkabani, Y. Perriard, and J.-J. Simond, "Power supply of long stator linear motors - application to multi mobile system," in *Industry Applications Society Annual Meeting, 2008. IAS '08. IEEE*, 2008, pp. 1–7.
- [11] K. Yoshida and X. Zhang, "Sensorless guidance control with constant airgap in ropeless linear elevator," in *The 4th International Power Electronics and Motion Control Conference*, vol. 2, 2004, pp. 772–776.
- [12] N. Takahashi, T. Yamada, D. Miyagi, and S. Markon, "Basic study of optimal design of linear motor for rope-less elevator," in *7th International Conference on Computation in Electromagnetics*, 2008, pp. 202–203.
- [13] K. B. Quan, H. X. Zhen, W. Hong-xing, and L. Li-yi, "Thrust and thermal characteristics of electromagnetic launcher based on permanent magnet linear synchronous motors," *Magnetics, IEEE Transactions on*, vol. 45, no. 1, pp. 358–362, 2009.
- [14] S. Markon, Y. Komatsu, A. Onat, A. Yamanaka, and E. Kazan, "Linear motor coils as brake actuators for multi-car elevators," in *Proc. LDIA*, 2007, pp. 73–74.
- [15] A. Onat, E. Kazan, N. Takahashi, D. Miyagi, and Y. Komatsu, "Design and implementation of a linear motor for multi-car elevators," *Mechatronics, IEEE Transactions on*, accepted for publication.
- [16] D. C. Meeker, "Finite element method magnets, version 4.2 (02nov2009 build)."
- [17] E. Kazan, "Design and implementation of a linear motor for multi-car elevators," Master's thesis, Sabanci University, Istanbul, Turkey, July 2009.
- [18] D. Nyce, *Linear Position Sensors: Theory and Application*. USA: Wiley Interscience, 2004.



Cagri Gurbuz Received his B.S. degree from Istanbul Technical University in 2008. He is currently studying as an M.S. student in mechatronics engineering at Sabanci University, Istanbul, Turkey. His current research interests are position sensing in linear synchronous motors and real-time communication issues in distributed linear motor control.



Ender Kazan Was born in Turkey in 1984. He received the B.S., and M.S. degrees in mechatronics engineering from Sabanci University, Istanbul, Turkey, in 2007, and 2009 respectively. He is currently with the Research and Development team of Desird Design R&D Co. Ltd., Istanbul, Turkey. His current research interests are microcomputer-based control of electric machines, and embedded system design.



Ahmet Onat Received his B.S degree in electronics from Istanbul Technical University in 1991, and Ms and PhD degrees in electrical engineering from Kyoto University, Japan, in 1995 and 1999 respectively. He is an Assistant Professor in Mechatronics at Sabanci University, Turkey since 2000. His current research interests include networked control systems and power electronics.



Sandor Markon Graduated from the Technical University of Budapest in 1973. Received Ph.D. in Electrical Engineering from Kyoto University in 1996. Researcher at Ganz Electric Works from 1973 to 1979, and at Fujitec Co., Ltd. from 1979 to 2008. Professor at Kobe Institute of Technology since 2004. Visiting researcher at the Japanese National Institute of Information and Communications Technology. Current professional interests include design, analysis, and control of linear motors, simulation and control of transportation systems, reliability of embedded software, and application of nanotechnology to optical imaging systems. Member of IEEE (Computer Society).